Adsorption (2010) 16: 3–15
DOI 10.1007/s10450-009-9203-8

PROCEEDINGS OF PBAST5

The role of accessibility in the characterization of porous solids and their adsorption properties

D.D. Do · L. Herrera · Chunyan Fan · A. Wongkoblap · D. Nicholson

Received: 30 July 2009 / Accepted: 19 November 2009 / Published online: 1 December 2009

Abstract This paper addresses the role of accessibility for adsorption in porous solids on the adsorption properties including Henry constant, adsorption isotherms and isosteric heat of adsorption. The relevant parameters are the accessible volume, the accessible geometrical surface area and the accessible pore size and its associated volume. This concept will be demonstrated to be important and calls for the need to consider adsorption characteristics in the most coherent and consistent manner. It is particularly reinforced by the limitations inherent in the conventional ways in determining the void volume, surface area and pore size. We provide a number of examples to support this; the challenge that faces us is the development of consistent experimental procedures to determine these accessible quantities. We define the accessible pore size as the size of the largest sphere that rests on three closest solid atoms in such a manner that any probe particle residing in that sphere would have a *non-positive solid-fluid potential* energy. For each accessible pore size there is an associated accessible pore volume, giving rise to a new accessible pore size distribution (APSD). This is distinct from the classical pore size distribution commonly used in the literature, and in our definition of accessible pore size, a zero pore size is possible. It is also emphasized that the accessible quantities that we introduce here are dependent on the choice of molecular probe, which is entirely consistent with the concept of molecular sieving.

Plenary Lecture at the 5th Pacific Basin Conference on Adsorption Science and Technology Singapore, 25–27 May 2009.

D.D. Do (✉) · L. Herrera · C. Fan · A. Wongkoblap · D. Nicholson
School of Chemical Engineering, University of Queensland, St. Lucia, Qld 4072, Australia
e-mail: d.d.do@uq.edu.au

Keywords Characterization · Accessibility · Porous solids · Gas adsorption · Pore volume · Pore size distribution

1 Introduction

Adsorption in porous solid has been used as a means to derive information about the pore volume, surface area and pore size (Gregg and Sing 1982; Rouquerol et al. 1999; Do 1998). The importance of gas phase adsorption in the characterization has been considered in a number of review papers (Kaneko et al. 2002; Do et al. 2007; Birkett and Do 2007). For simplicity nitrogen and argon are among the commonly used molecular probes for this purpose, and are recommended as a suitable probe for the determination of structural parameters of porous solids (Sing et al. 1985; Rouquerol et al. 1994). Indeed a number of reviews have been presented in the literature, dealing almost exclusively with these simple molecular probes (Kaneko 1994; Kaneko et al. 1998b; Thommes et al. 2000; Thommes 2004; Do et al. 2008a). With the recent discovery of well defined mesoporous solids such as MCM-41, SBA-15, SBA-16, etc., there has been a surge of interest in characterization with numerous papers on experimental, theoretical and simulation aspects of characterization (Kruk and Jaroniec 2000; Kowalczyk et al. 2005; Ustinov et al. 2005, 2006; Thommes et al. 2006; Jaroniec et al. 1999; Kruk and Jaroniec 2003). Classical theories such as the BJH method (Barrett et al. 1951; Jaroniec et al. 2002), the Broekhoff and de Boer (BdB) theory (Broekhoff and de Boer 1967, 1968a, 1968b; Ustinov et al. 2005), the Cole and Saam (CS) theory (Cole and Saam 1974) have been challenged by modern methods that have a basis in statistical mechanics (Thommes et al. 2006; Kanda et al. 2000; Neimark et al. 1998, 2003; Visnyakov

and Neimark 2003; Ravikovitch and Neimark 2001, 2002; Neimark and Ravikovitch 2001; Ravikovitch et al. 1995, 1998, 2000).

Let us now discuss these structural quantities. The adsorptive capacity of a porous solid is governed by the void volume (particularly for sub-critical conditions), and this volume has been determined in a number of ways (Gregg and Sing 1982; Rouquerol et al. 1999). One is the helium expansion method and another is the adsorption of some molecular probe at its boiling point. Since pores of most practical solids are of molecular dimension, what do the volumes obtained by these methods refer to? In Sect. 2, we show that neither of these volumes is useful in characterizing adsorption in a consistent manner. Surface area is traditionally determined by the BET method, although there are a number of suggestions to use other means for this purpose (Neimark and Ravikovitch 1997; Do and Do 2005a, 2005b). The continuing use of the BET method as a routine tool to obtain surface area persists because of its simplicity and because the other alternatives involve extra computations or lengthier experimental procedures. If the BET method is meant to provide the geometrical surface area, it falls short of the goal because of the assumptions inherent in the theory. We support this view with detailed molecular simulation in Sect. 3. Finally we discuss the pore size. To determine the pore size, one has to resort to a specific pore geometry. Very often a slit model or a cylinder model is assumed, and if a spherical cage is expected then a spherical model is used. With these assumptions, the derived pore size distribution is model-dependent. Among the three structural quantities, surface area, void volume and pore size, this last is the most difficult one to define.

In this paper we propose a means of analyzing an adsorption system with the goal of deriving the surface area, void volume and pore size in a consistent manner. The key concept here is the accessibility and we will show that by adopting the accessible surface area, accessible void volume and accessible pore size (and accessible pore size distribution) we can present adsorption in a manner which is transparent. To lay a foundation we illustrate this concept of accessibility with model solids whose atomic configurations are known, i.e. ones in which we know the positions of all solid atoms in the porous solid. We shall use Monte Carlo integration for the determination of the structural quantities.

2 Accessible volume

We first briefly discuss the importance of the accessible volume in the calculation of the Henry constant and the isosteric heat at zero loading. Details of this analysis are given in Do et al. (2008c, 2008d, 2008e, 2009). For a given volume, Ω, containing solid atoms and void space in which adsorption is taking place, the interaction energy between a fluid particle placed at a point $\underline{r}$ and all solid atoms be $\phi(\underline{r})$. Under very dilute conditions, the adsorption is low enough that the potential energy of the system is entirely due to the solid-fluid interaction and the local density at any point $\underline{r}$ is related to the bulk gas density by the Boltzmann distribution law (Steele and Halsey 1955; Barker and Everett 1962), $\rho(\underline{r}) = \rho_b \exp[-\phi(\underline{r})/kT]$, where ρ_b is the bulk gas density. Therefore, the total number of particles that can be found in the volume Ω is merely the volume integration of that local density, as shown below

$$N = \rho_b \int_\Omega \exp[-\phi(\underline{r})/kT] d\underline{r} \tag{1}$$

This equation is generally valid as long as there is no clustering among fluid particles.[1] For the purpose of determining the amount adsorbed we refer to the excess amount, which is defined as the difference between the total amount in the volume Ω (which is (1)) and the amount that would occupy the void volume at the density which is the same as the bulk phase density. By this definition the excess amount is:

$$N_{ex} = \rho_b \int_\Omega \exp[-\phi(\underline{r})/kT] d\underline{r} - V_{void}\rho_b \tag{2}$$

Thus the excess amount is a calculated quantity, not a measurable one because it depends on the way we define the void volume, V_{void}. This is where the difficulty arises. Let us show what we mean. Helium is commonly used to measure void volume, and this is done by dosing a known amount of helium, N_{He}, into the volume Ω at T_{He} at which the system is dilute. We have, by virtue of (1), a relationship between the amount dosed and the uniform density of helium far away from the surface, ρ_{He}:

$$N_{He} = \rho_{He} \int_\Omega \exp[-\phi_{He}(\underline{r})/kT_{He}] d\underline{r} \tag{3}$$

where ϕ_{He} is the helium-solid potential energy. If we define the void volume as that in which the helium density is equal to ρ_{He} everywhere in that volume (i.e. zero excess amount for helium), we have

$$V_{void} = (N_{He}/\rho_{He}) \tag{4}$$

where N_{He} is given in (3). Clearly this void volume is *greater* than the "geometrical" void volume because of the enhancement in the helium density in the regions close to the surface where ϕ_{He} is negative. To show that this void volume over-estimates the geometrical volume of the pore, we take an example of a graphitic slit pore whose physical width is 7 A. The width is defined as the distance between

[1] We exclude strongly associating fluids as they tend to form clusters even in the most dilute conditions of the gaseous phase. Water is an outstanding example.

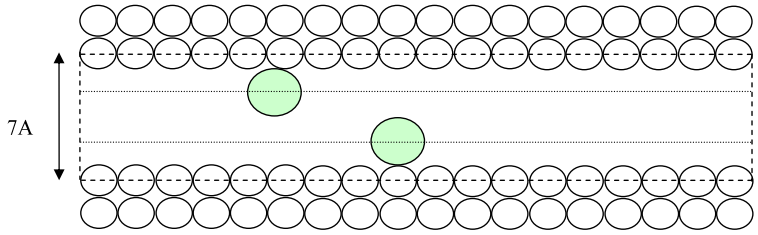

Fig. 1 Schematic diagram of a graphitic slit pore. The physical width is 7 A. The absolute volume is bounded by the *dashed line*, passing through the outermost layer of the walls. The accessible volume is bounded by the *dotted line*, in which the solid-fluid potential energy is non-positive

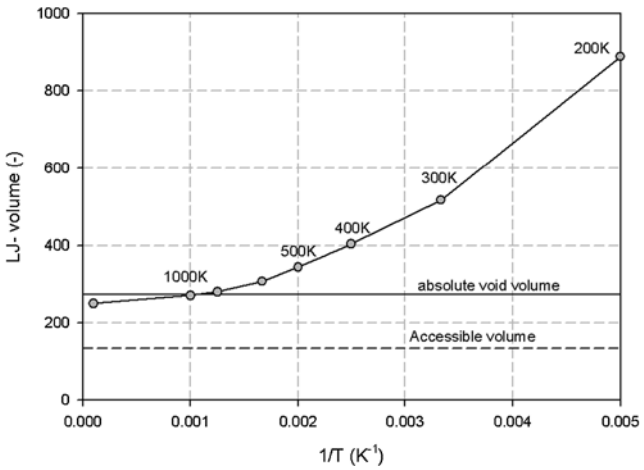

Fig. 2 Plot of the LJ-volume obtained with helium adsorption in a 7 A graphitic slit pore

Table 1 Saturation vapour pressure and liquid density of argon obtained from the Gibbs ensemble MC

T (K)	Saturation vapour pressure (Pa)	Saturation liquid density (mol/m^3)
77	33.53	36,419
87.3	100.2	35,060
90	117.6	34,509
100	258	32,960
120	1048	29,398
130	1759	27,306
140	2788	25,129
150	3942	20,857

a plane passing through the centres of carbon atoms in the outermost layer of one wall and the corresponding plane on the opposite wall (see Fig. 1).

We carry out the Monte Carlo integration of (4) at various temperatures, with helium as the adsorbate in this pore having a linear dimension in the x- and y-directions of 15 times the collision diameter. Helium is treated as a single LJ-particle with a collision diameter of 0.2556 nm and a reduced well depth of the fluid-fluid interaction energy of 10.22 K. The solid-fluid potential energy is calculated with Steele 10-4-3 equation with the following molecular parameters for carbon atom in the graphene layer, $\sigma_{ss} = 0.34$ nm and $\varepsilon_{ss}/k_B = 28$ K. The bulk pressure is fixed at 1 atmosphere. We plot in Fig. 2 the LJ-volume calculated from (4), $V_{void}\sigma_{ff}^3$ (which is dimensionless), as a function of the inverse of temperature. Also plotted in this figure are the absolute void volume and the accessible volume. The former is defined as the volume bounded by the planes passing through the carbon atoms of the outermost layer (shown as dashed line in Fig. 1), while the accessible volume is defined as the region in which the solid-fluid potential energy is non-positive (shown as the dotted line). If either of these volumes is taken to be the representative volume of this 7 A graphitic slit pore, we see that the He-void volume does not describe any of them correctly. For temperatures less than 1000 K the void volume calculated by the helium expansion is much greater than either the absolute volume or the accessible volume.

Another way to determine the void volume is to carry out adsorption at pressures close to the saturation vapour pressure so that all void space would be filled with adsorbate molecules. By assuming that the average density of the adsorbed phase is the same as the liquid density (a questionable assumption), the void volume is obtained. We call this the adsorption saturation volume. Typically this is done with argon adsorption. To show whether this will fare any better than what we have seen earlier with helium expansion in Fig. 2, we carry out a GCMC molecular simulation of argon adsorption in the same pore, a 7 A graphitic slit pore, at a number of temperatures below the critical temperature. The box length in the x- and y-directions is taken to be 10 times the collision diameter of argon. The molecular parameters of argon are $\sigma_{ff} = 0.3405$ nm and $\varepsilon_{ff}/k_B = 119.8$ K. The saturation vapour pressure and the saturation liquid density at each temperature for this potential model of argon were obtained from a Gibbs ensemble Monte Carlo simulation. The results of this simulation are shown in Table 1.

Let N be the ensemble average from the GCMC simulation at the saturation vapour pressure corresponding to a

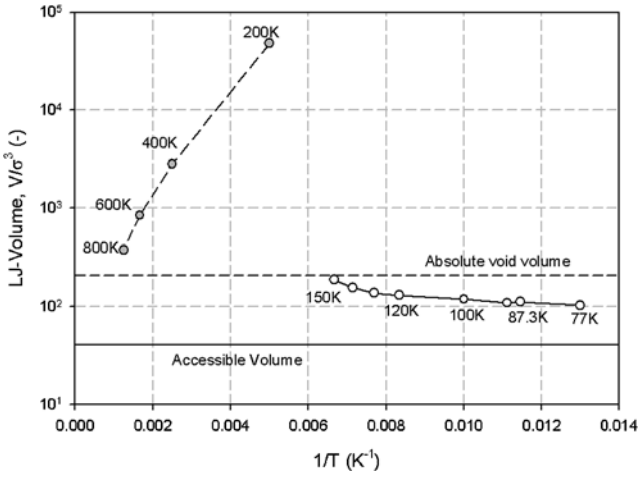

Fig. 3 Plot of the void volume versus the inverse of temperature for argon adsorption in a graphitic slit pore of 7 A width

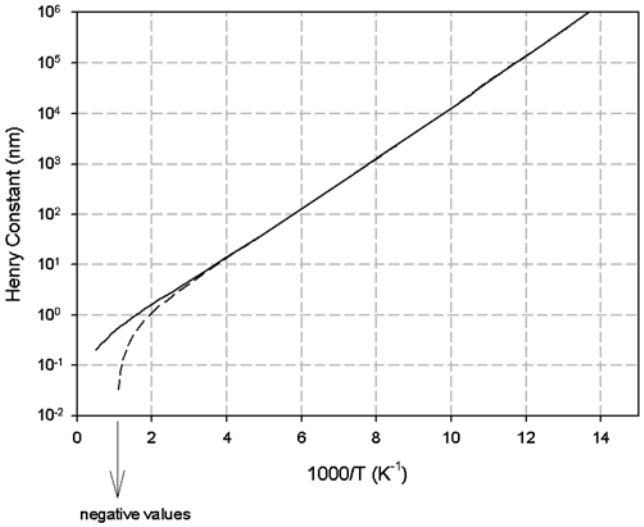

Fig. 4 Plot of the Henry constant (logarithmic scale; base 10) versus the inverse of temperature for argon adsorption inside a single carbon nanotube of radius 0.949 nm (the radius is defined as the distance between the centre of the tube to the circle passing through the centres of carbon atoms on the surface of the carbon nanotube). The *full line* is calculated using accessible volume, the *dashed line* shows the Henry constant calculated from (7)

given temperature in Table 1. We calculate the void volume of the pore from the following equation:

$$V_{\text{void}} = \frac{N}{\rho_{\text{L}}} \tag{5}$$

where ρ_{L} is the saturation liquid density. Figure 3 shows the reduced LJ-void volume $V_{\text{void}}\sigma^3$calculated using (5), as a function temperature in the subcritical range (shown as solid line). The absolute volume and the accessible volume are also plotted in this figure. We see that this void volume again does not describe either of these geometrical volumes. For comparison, we also show in this plot the volume obtained using (4) with argon as the adsorbate in place of helium. This is shown as dashed line for argon expansion at 100 kPa and a number of temperatures above the critical point. Obviously this void volume with argon expansion is much greater than either the absolute volume or the accessible volume because the polarizability of argon is much greater than that of helium.

Such a wide variation in the void volume from the expansion at temperatures greater than the critical point (4) and the adsorption saturation volume for temperatures less than the critical point (5) calls for a need to define a volume that is more suitable for adsorption calculations. We argue that this volume is the accessible volume. It is defined as the volume in which the fluid-solid interaction energy of a particle placed anywhere in that volume is non-positive. In this definition, the boundary of this volume is the loci of positions at which the fluid-solid potential energy is zero.

Having seen that neither the void volume from the expansion at temperatures greater than the critical point nor the adsorption saturation volume calculated for temperatures less than the critical point can provide us with a proper void volume, we turn our attention to the accessible void volume and present our case in using this as the fundamental volume to calculate adsorption properties. The question that one has to raise is: how would one benefit from this accessible volume, should we decide to use it? Do et al. (2008b, 2008c) have shown that by using the accessible volume the Henry constant is always positive (which should be the case if one would expect it to have physical significance). The surface excess of adsorption of argon on a graphitic surface is calculated from:

$$\Gamma = \frac{N_{\text{ex}}}{A} = \frac{1}{A}\left[\int_{\Omega} \exp[-\phi(\underline{r})/kT]d\underline{r} - V_{\text{void}}\right]\rho_{\text{b}} \tag{6}$$

from which the Henry constant is:

$$K = \frac{\Gamma}{\rho_{\text{b}}} = \frac{1}{A}\left[\int_{\Omega} \exp[-\phi(\underline{r})/kT]d\underline{r} - V_{\text{void}}\right] \tag{7}$$

when the void volume in the above equation is taken to be the accessible volume, the Henry constant is always positive for all temperatures investigated. This is shown in Fig. 4 for argon adsorption in a single carbon nanotube of radius 0.949 nm, where we plot the logarithm of the Henry constant as a function of the inverse of temperature. On the other hand, if we use the absolute volume from (7), the Henry constant becomes negative at high temperatures. Since we cannot show negative values on a log plot, we indicate this with the arrow as shown in Fig. 4. Although the Henry constant at high temperatures is not so relevant because physical adsorption is rarely carried out at these temperatures, we have to be consistent with the way we define our physical quantities. The accessible volume meets this criterion.

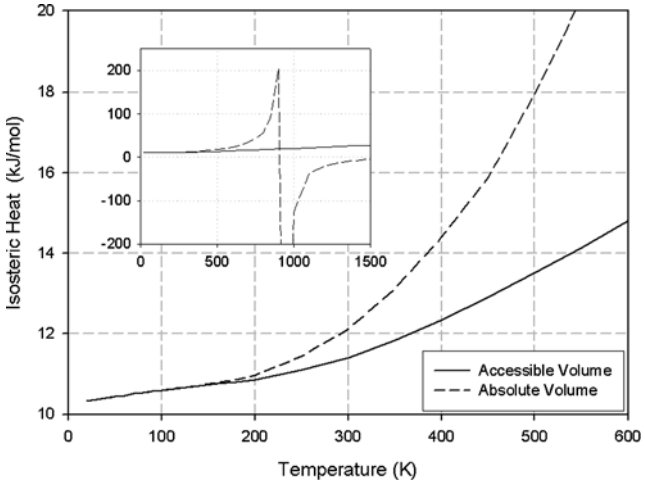

Fig. 5 Isosteric heat at zero loading versus temperature for argon adsorption inside a single carbon nanotube of radius 0.949 nm. *The inset* shows the isosteric heat over a wider range of temperature

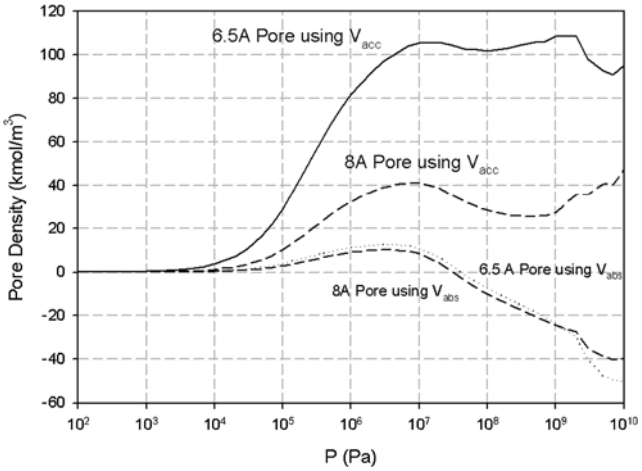

Fig. 6 Excess density for adsorption of argon in graphitic slit pores having widths 6.5 and 8 A at 273 K

A further support of the use of the accessible volume is the calculation of the isosteric heat at zero loading. Although isosteric heat has been used constantly in the literature in the calculation of the amount of heat released per unit change in the particle added to the adsorbed phase, it has been used almost in a mechanical manner. A derivation for the isosteric heat at zero loading in the grand canonical ensemble has been provided by Do et al. (2008b).

$$q_{\mathrm{st,ex}}^{(0)} = kT - kT\frac{\int_{\Omega}[\phi(\underline{r})/kT]\exp[-\phi(\underline{r})/kT]d\underline{r}}{\int_{\Omega}\exp[-\phi(\underline{r})/kT]d\underline{r} - V_{\mathrm{void}}} \tag{8}$$

Figure 5 shows the plot of the isosteric heat at zero loading versus temperature for adsorption of argon inside a single carbon nanotube (Do et al. 2008c). It is seen that the heat calculated using the helium void volume (inset) at high temperatures is too high to be physically realistic and it even becomes negative for higher temperatures. The heat calculated using the accessible volume is always finite and remains within the range that one would expect for physical adsorption.

We have demonstrated that the accessible volume is the best choice to use in adsorption studies. As a further support to this we now illustrate its utility in the calculation of the excess density for supercritical adsorption. The excess density is defined as:

$$\rho_{\mathrm{ex}} = (N - V_{\mathrm{void}}\rho_{\mathrm{b}})/m \tag{9}$$

It is known in the literature that the surface excess has a maximum density and can become negative at high pressures. A negative excess density implies that the density in the bulk phase is greater than that inside the porous solid. While this might seem possible at extremely high pressures at which the confinement effects could prevent an optimal packing in the adsorbate, it is difficult to accept this negative quantity physically. The reason for this negativity is because of the use of helium volume as the void volume in the calculation of the excess density. The problems associated with the use of helium in the determination of void volume have already been addressed in Do and Do (2007), Neimark and Ravikovitch (1997). Yet again we argue that if we use the accessible volume in the calculation of the excess density we will have positive excess density, and indeed this is the case as seen in Fig. 6 where we show the excess density for argon adsorption in graphitic slit pores of widths 6.5 and 8 A. The width is defined as the distance from the plane passing through the centres of all carbon atoms of the outermost layer of one wall to the corresponding plane of the other wall.

We see that by using the accessible volume to calculate the excess density the results are always positive. On the other hand the excess density calculated using the absolute void volume becomes negative at pressures greater than 20 MPa (which is about 200 atm). It is difficult to accept at this pressure that the bulk density is denser than the density inside the pores where one would expect that the surface forces should density the adsorbed phase!

We have shown and argued that the accessible volume is the fundamental variable to use in adsorption studies. Its use moreover allows us to strengthen the meaning of molecular sieving because the accessible volume is different for different adsorbates. As a general rule, the smaller the molecular probe the large the accessible volume, which depends on the adsorbate-solid interaction potential and the average orientation that the adsorbate presents to the adsorbent at a given T.

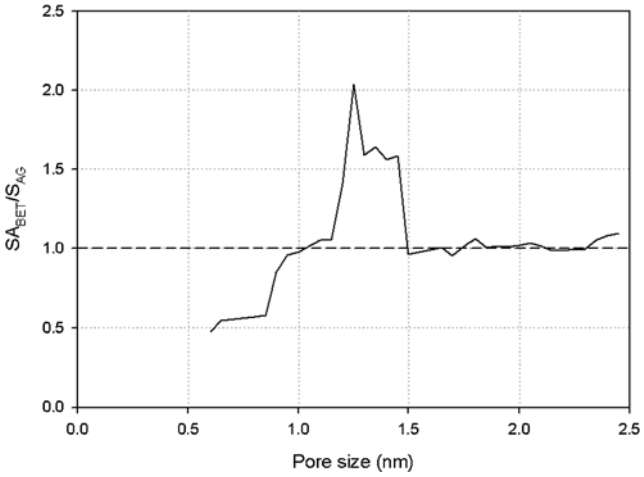

Fig. 7 Plot of the ratio of the BET surface area to the geometrical area for model slit pores of various sizes

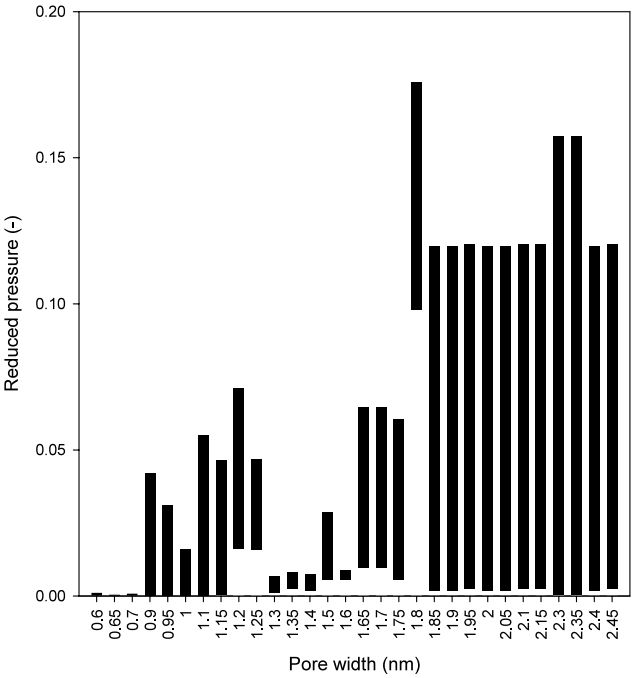

Fig. 8 Range of pressures used to calculate the BET surface area according to the pore size

3 Accessible geometrical surface area

We now address the surface area of a solid. Although there are some alternatives in the determination of surface area, the BET method remains the method of choice, primarily because of its simplicity. It has been known for a very long time, since the theory was firs proposed by Brunauer et al. (1938), that its validity is limited to surfaces with small curvature and its application to surfaces with high curvature or in pores of solid dimensions is questionable (Gregg and Sing 1982; Rouquerol et al. 1999). By carrying the Grand Canonical Monte Carlo simulation in slit pores of various sizes and applying the BET method to the simulated isotherm data, we can obtain the BET surface area and compare it directly against the geometrical surface area. Our slit pore model is the homogeneous graphitic pore, modelled with the Steele 10-4-3 potential model. Therefore the accessible geometrical surface area is simply twice the area of one wall, $A_{\text{acc}} = 2L_xL_y$, where L_x and L_y are the linear dimensions of the simulation box.

The results are shown in Fig. 7 where we plot the ratio of the BET area to the geometrical area versus the pore width. In Fig. 8 we show the range of reduced pressures for the linearity of the BET plot used for each pore size. These pressure ranges were selected according to the suggestion of Rouquerol et al. (2007).

For large pores we expect that the BET surface area is comparable to the geometrical area. The same can not be said for smaller pores where we see that the BET surface area can be either greater or smaller than the true geometrical area. For a slit pore of width of 1 nm, the two areas are the same because this pore can pack exactly two molecular layers and hence two units of BET area (by virtue of two molecular layers) indeed correspond to two units of geometrical surface area. For pores smaller than 1 nm only about one layer can be accommodated but there are two units of geometrical area, and therefore the BET surface area underestimates the geometrical area. On the other hand, for slit pores having width greater than 1 nm, the BET surface area over-estimates the geometrical area because three or four layers can be packed in this pore and therefore the BET area can be as high as twice the geometrical area (see the highest peak in Fig. 7). This simple example serves as an illustration to show that one should treat the BET surface area only as a guide on how large a surface is. Its use in comparing two different solids should also treated with care.

In previous work (Duren et al. 2007), a "rolling van der Waals sphere" has been employed as a probe to determine surface area and the merits of this procedure compared with other proposals such as the Conolly or van der Waals surface areas. If the rolling sphere probe interacts with each surface atom through an L-J potential φ_{LJ}, and the hard sphere separation of probe and adsorbent atom is σ, then the rolling sphere is, in effect a solution to the equation $\varphi_{\text{LJ}} = 0$. Our accessible surface, in contrast, is a solution to the equation $\varphi_{\text{ads}}(\boldsymbol{r}) = 0$ where φ_{ads} is the adsorption potential at $\boldsymbol{r}$, calculated from the interaction of the probe with the whole adsorbent.

4 Accessible pore size

When one needs to determine the pore size of a given solid, more often than not a geometrical model must be chosen.

For example, one has to decide the pore geometry to take either slit, cylinder or sphere. This is indeed the case in almost all methods used in the literature to determine the pore size and its distribution. Once a choice for the pore shape has been made, one simply obtains a set of adsorption isotherms for pores of various sizes. This set is called the kernel and this kernel is then used in an integral equation (assuming patchwise configuration of pores, that is pores of the same size are grouped together and there is no interaction between these groups) to derive the pore size distribution. The integral equation relating the observed density (mol/kg) to the local adsorption isotherms is as follows

$$\rho_{\exp}(p) = \int \rho(p; H) f(H) dH \tag{10}$$

where $\rho(p; H)$ is the local adsorption isotherm (mol/m^3) and is a member of the kernel, and $f(H)$ is the pore size distribution with $f(H)dH$ is the volume per unit mass for pores having sizes falling between H and $H + dH$. The problem is known as an ill-posed problem and discussions of this issue have been addressed in Tikhonov and Arsenin (1977).

Unfortunately pores of real solids rarely conform to any simple shape. Metal organic frameworks are an example where pores do not resemble slit, cylinder or sphere. Therefore there is a need to develop a means to determine the pore size for an arbitrary solid, and this is what we will show next. The accessible pore size that we are proposing here has the low limit of zero. In other words zero accessible pore size is possible. Take a simple slit pore with homogeneous walls as an example. The size of this pore is chosen such that the solid-fluid potential is positive everywhere except at the centre where it is zero (Fig. 9). By our definition, this pore has zero accessible volume and zero accessible pore size. This is an absolute lower limit of pore size.

Could zero volume give an infinite adsorbed density? Even though the accessible pore volume is zero, the number of particles adsorbed in this pore is *also* zero by virtue of $\phi > 0$ in (1). Since the number of particles approaches zero much faster than the pore volume, because of the strong repulsion in ultra-fine pores, the pore density, calculated as number of particles per unit accessible volume, approaches zero in the limit when the accessible pore size approaches zero. We illustrate this with a plot of the accessible pore density versus the *accessible* pore size for argon adsorption in graphitic slit pores at 87.3 K (Do et al. 2008f) (Fig. 10). It is seen that the pore density increases as the pore size is decreased. It reaches a maximum and then decreases very sharply because of the strong repulsion to the point that we can clearly see a sieving effect. This once again reiterates the significance of the use of the accessibility concept where the molecular sieving can be manifested. For comparison we also show the plot of pore density versus the *physical* pore size (which is defined as the distance between the plane

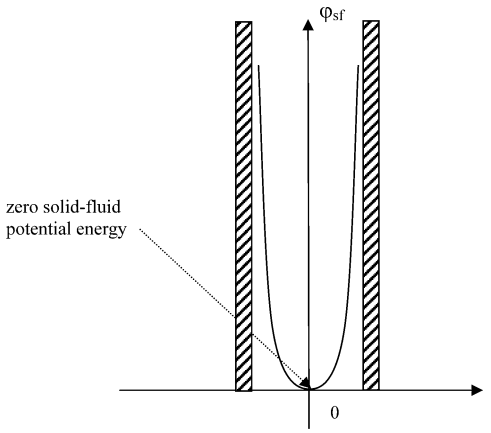

Fig. 9 A perfect slit pore with zero accessible volume and zero accessible pore radius

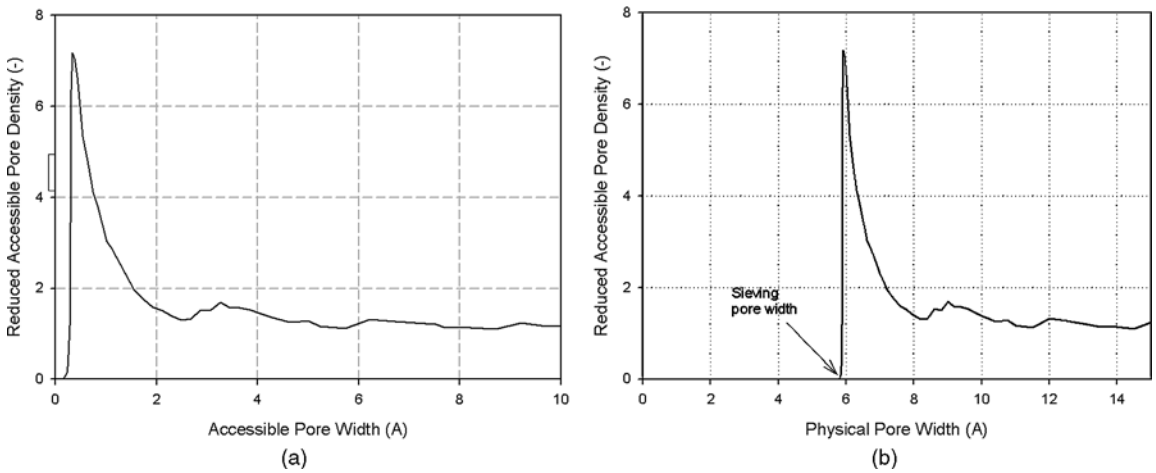

Fig. 10 (**a**) Plot of accessible pore density versus accessible pore width for argon adsorption in graphitic slit pores at 87.3 K; (**b**) Plot of accessible pore density versus physical pore width for the same system

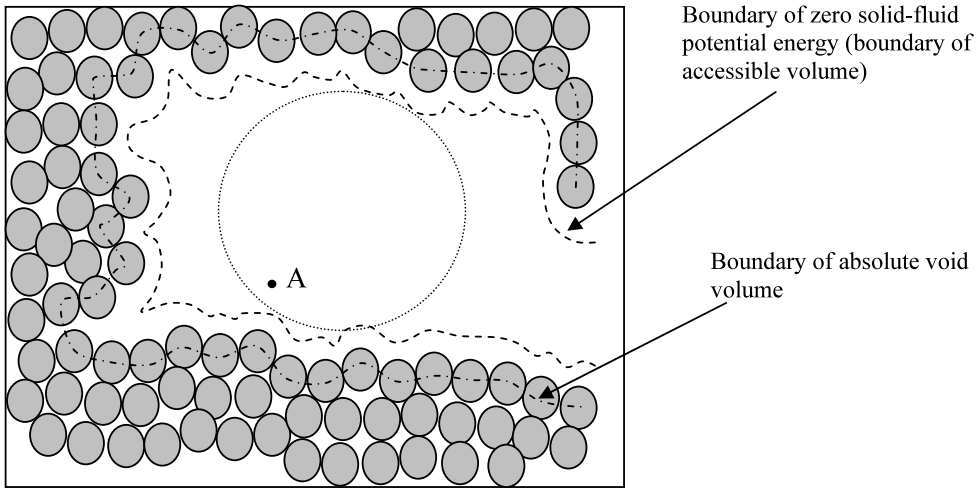

Fig. 11 Schematic diagram of a porous solid

passing through the centres of carbon atoms of the outermost layer of one wall and the corresponding plane of the opposite wall). This plot shows that the physical width for the sieving of argon is 5.89 A. If we do this for the larger xenon probe, the sieving width is 6.46 A. What this simply means is that argon can access pores in the range from 5.89 to 6.46 A, whereas xenon cannot.

Unlike the accessible pore volume and the accessible geometrical area, which are macroscopic quantities, the accessible pore size is a local quantity. It depends on the location inside the pore. Of course, only the location that has non-positive solid-fluid potential is considered, that is we only consider the locations inside the accessible volume. For each legitimate position, say point A, chosen inside the accessible volume, the accessible pore size is defined as the size of the largest sphere that one can find such that this sphere satisfies the following criteria:

1. The point A is within the sphere or on its surface
2. A molecular probe residing on any point on the surface of this sphere would have non-positive solid potential energy
3. This sphere, in general, has three solid atoms such that $\phi = 0$.

Because of this last property of the sphere, we shall describe this as the Tri-POD method. Details of this accessible pore size for some well defined pores are provided in Do and Do (2007), Do et al. (2008f, 2008g), Do (2008), Herrera et al. (2009). For an arbitrary solid with known solid atom configuration, how do we determine an accessible pore size and the accessible volume associated with this pore size? The answer rests on the way we determine the total accessible volume. By making an insertion of a particle at a point chosen at random, $\underline{r}$, we compute the solid-fluid potential energy between the particle and all solid atoms, $\varphi(\underline{r})$. If this potential energy is non-positive, this insertion is a success and therefore contributes to the total accessible volume. This process, when repeated M times (usually of the order of one million), will give a success fraction f, and the total accessible volume is calculated from $V_{\text{acc}} = \sum_{j=1}^{M} f \times \delta V$, where the differential volume is equal to the volume of the simulation box divided by M, i.e. $\delta V = V_{\text{box}}/M$, because we sample the space of the simulation box with equal probability. Therefore, the above equation becomes $V_{\text{acc}} = f \times V_{\text{box}}$. The next step is to determine the accessible pore size each time we make a successful insertion. If the insertion is successful, we have to determine the pore size corresponding to this insertion point $\underline{r}$ and then the differential volume of this insertion, δV, will be counted towards this pore size. If the point A is chosen at random (Fig. 11) and its solid-fluid potential energy is non-positive (i.e. successful insertion), we search for a largest sphere that encloses this point and rests on three closest solid atoms such that any molecular probe residing inside this sphere will have a non-positive solid-fluid potential energy (shown as a dotted line in Fig. 11). Let the diameter of this sphere be D_j, then the volume associated with this pore size is incremented by δV. It is noted that for M insertions at random, each insertion point $\underline{r}$ (having a differential volume of V/M) is associated with a particular size.

To calculate the PSD, we repeat this process M times, and at each successful insertion we determine the pore size in the manner just described. The accessible volume corresponding to the pore size D_j is simply calculated from $V_{\text{acc},j} = \sum_{j=1}^{M_j} \delta V$, where the variable M_j is the number of successful insertions that have a pore size of D_j. Since $\delta V = V_{\text{box}}/M$, this equation becomes $V_{\text{acc},j} = (M_j/M)V_{\text{box}}$. It is clear that $f = \sum_j M_j/M$ and therefore, $V_{\text{acc}} = \sum_j V_{\text{acc},j}$. That is the sum of all the individual accessible volumes corresponding to all pore sizes is equal to the total accessible volume, and the relationship between the accessible pore size D_j and the individual accessible volume $V_{\text{acc},j}$ is the pore size distribution. To distinguish our new definition

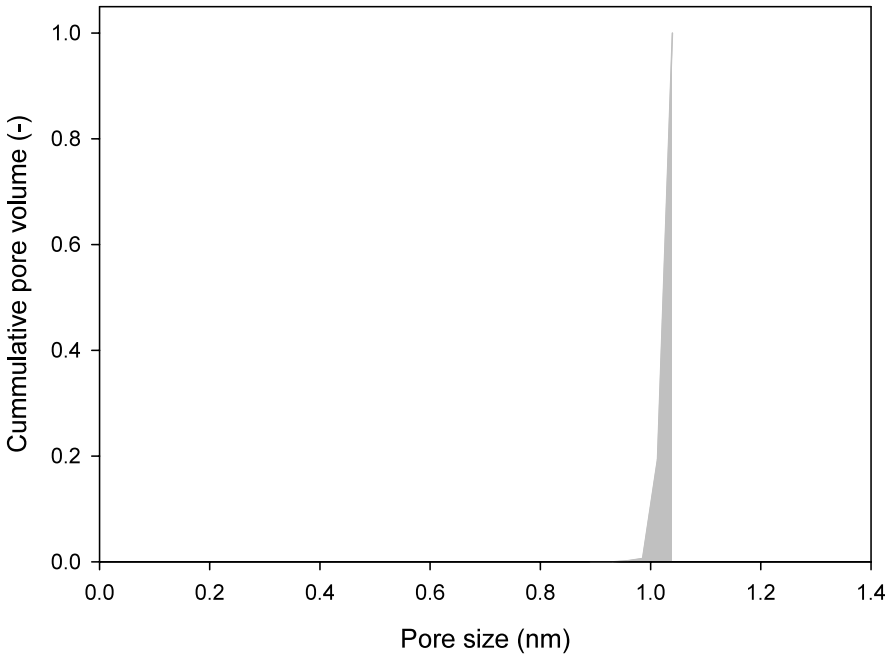

Fig. 12 The accessible pore size distribution (APSD) of slit pore of 1.562 nm physical width

of pore size distribution (PSD) from the traditional PSD, we coin ours the accessible pore size distribution (APSD). A method in which probing spheres were used as a basis for defining pore size distributions has also been used by Gelb and Gubbins (1999), but these authors did not employ an accessible volume approach, nor the Tri-POD concept that is central to the scheme proposed here.

Having defined the concept of the accessible pore size and APSD, we now turn to the determination of the APSDs of some model solids—slit pore, defective slit pore, metal organic frame works (MOF5) and the zeolite Li-ABW. The APSDs are calculated with argon as a probe molecule whose collision diameter is 0.3405 nm.

4.1 Slit pore

To check on the validity of the method to determine accessible pore size and its distribution with respect to the accessible volume, we apply the method to the graphitic slit pore whose walls are made up of graphene layers (Kaneko et al. 1998a). The two walls are composed of carbon atoms having a collision diameter of 0.34 nm, and the distance between two adjacent carbon atoms is 0.142 nm. The physical pore width is 1.562 nm (distance between the two planes passing through the centers of carbon atoms at the outermost layers). Using Monte Carlo integration, the total accessible volume is found to be 0.30 cm^3/g, and the cumulative pore volume distribution is shown in Fig. 12. The figure shows a peak around 1.01 nm accessible pore size, which is the expected peak as one would derive from the knowledge of the analytical solid-fluid potential energy profile. Beside this major peak at 1.01 nm, we see that the distribution develops from about 0.96 nm, which is due to the corrugation of the graphene layers.

4.2 Defective pore

We now consider a defective graphitic slit pore to see how the cumulative pore volume varies with the defects on the graphene layer. This pore is constructed by starting with a graphitic slit pore with two perfect graphene layers in each wall and two defective inner layers. The defective layers are made by selecting a carbon atom at random and then removing it together with its neighboring carbon atoms that fall within a specified radius. This process is repeated until a certain defect percentage is achieved. Here a defect radius of 0.492 nm and the defect percentage of 50% are used. The other geometrical parameters of this defective pore are H, L_x and L_y equal to 2.2, 4.6 and 4.4 nm, respectively. Giving these parameters, the total accessible volume obtained from the Monte Carlo integration is 0.494 cm^3/g and the cumulative pore volume is shown in Fig. 13. This figure shows a population of pores having pores up to 1 nm. These pores are from the small spaces around the defects. The cumulative volume has a sudden increase at a pore size of 1 nm. This is contributed by the pore space between the two parallel defective layers (pores between 1.0 and 1.2 nm in the figure). The largest pores (pore sizes greater than 1.25 nm) are from the volume between the perfect graphene layers.

4.3 Metal organic framework (MOF)

Next we consider one example of the metal organic frameworks (MOF) that have received much attention in recent

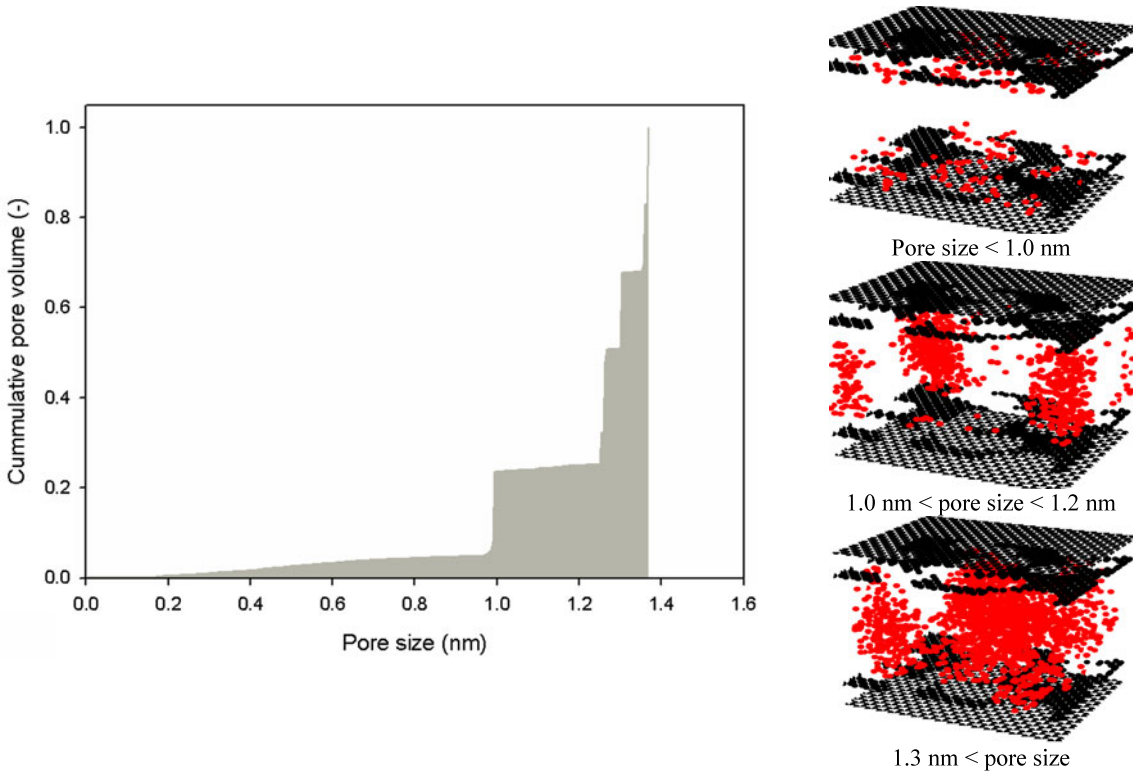

Fig. 13 The accessible pore size distribution (APSD) of a defective slit pore whose dimensions and properties are given in the text

Fig. 14 (Color online) Schematic diagram of the MOF-5 and its APSD, (*light gray*) hydrogen, (*gray*) carbon, (*red*) oxygen and (*pink*) zinc. The figures show the insertion points for the pore sizes indicated

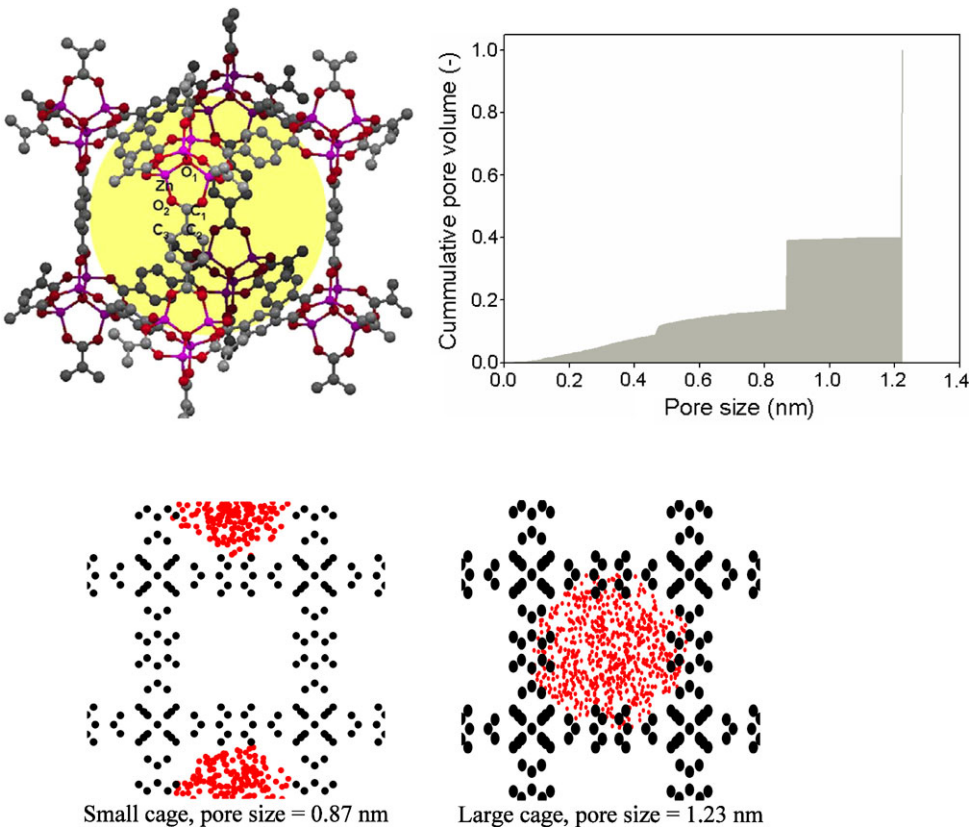

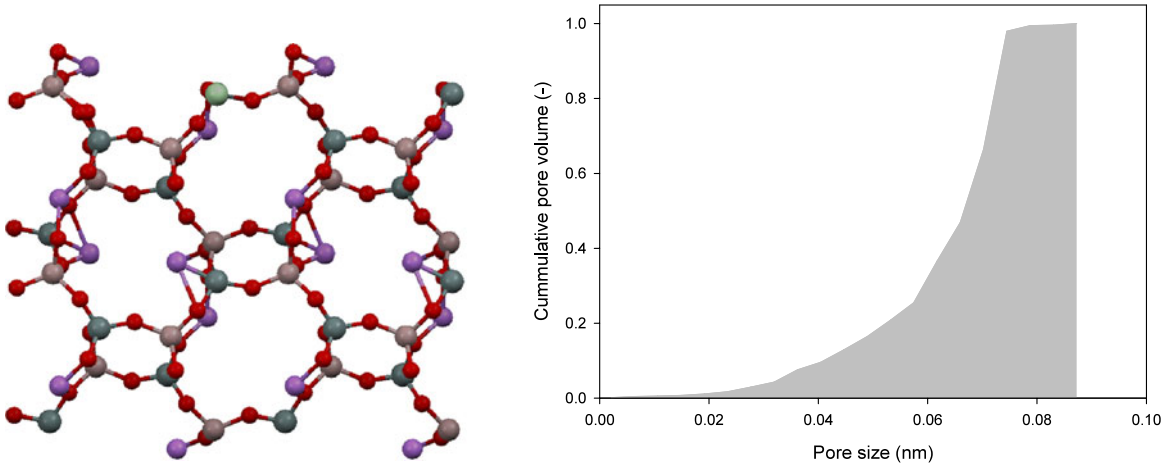

Fig. 15 Schematic diagram of the Li-ABW zeolite and its cumulative pore volume

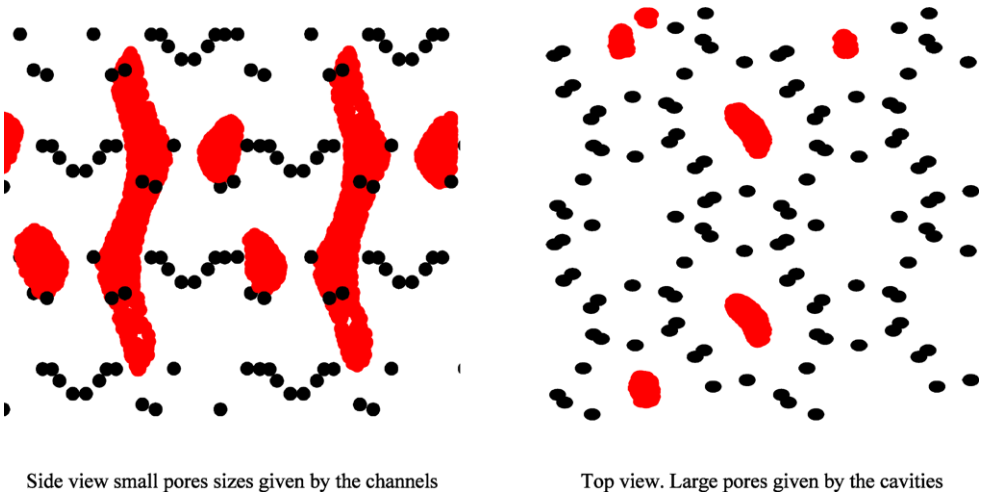

Fig. 16 Schematic diagram of the small and large pores in the Li-ABW zeolite

Table 2 Geometry parameters of MOF-5

	Bond (nm)		Angle (°)
O1-Zn	0.1968	Zn-O2-C1	130.7
Zn-O2	0.1947	O2-C1-O2	127.2
O2-C1	0.1254	O2-C1-C2	116.4
C1-C2	0.1515	C1-C2-C3	120.1
C2-C3	0.1381	C2-C3-H	119.5
C3-C4	0.1381		
C3-H	0.1108		

Table 3 Atomic coordinates for Li-ABW zeolite

	x	*y*	*z*
Li	1862	6849	2520
Al	1593	810	2500
Si	3544	3757	2492
O1	65	1584	1970
O2	2736	2198	1391
O3	1912	399	5907
O4	1804	−1008	689
O5	5891	903	−2395

years. We take MOF-5, which is also known as IRMOF-1, as one typical example. This MOF is a porous cubic crystal formed by the connection between a Zn_4O and benzene-1,4-dicarboxylate (Eddaoudi et al. 2002) (Fig. 14). MOF-5 is characterized by two different cavities formed by the two different orientations of the ligands in the structure. The computed lattice parameters are taken from Walton and Snurr (2007) and listed in Table 2. From the Monte Carlo integration, we find that the argon accessible pore volume is 0.825 cm^3/g and the cumulative pore volume is shown in Fig. 14. The figure shows that for pore sizes less than 0.85 nm there is a slow increment in the pore volume, this is because of the effect of the corners and windows in the structure. Then for pores around 0.87 nm there is a sudden increase in the pore volume up to 0.42, this sudden incre-

ment is due to the volume of the small cavity. After this a second increment appears for a pore size of 1.23 nm. This is due to the largest cavity of the structure. These two sizes for the small and larger cavities agree with the result obtained by Eddaoudi et al. (2002).

4.4 Zeolite

Finally we show an example of Li-ABW zeolite (Szostak 1992; Reed and Breck 1956). Its structure is shown in Fig. 15 as well as its APSD. The zeolite is an orthorhombic structure with pores of 0.34×0.38 nm. Its structure was developed based on the crystal parameter Pna21, and the unit cell $a = 1.0313$, $b = 0.8194$ and $c = 0.4993$ nm with angles $\alpha = \beta = \gamma = 90$. The atomic coordinates of this zeolite are shown in Table 3.

The total argon accessible volume of this zeolite is 0.002 cm^3/g. The cumulative pore volume shows an initial increment in the pore volume given by the small pores sizes from the channels in the zeolite (LHS in Fig. 16) then the cumulative pore volume level off for a pore size of 0.074 nm. These pores come from the main cage of the zeolite (RHS in Fig. 16) and this agrees with the pore size reported in Szostak (1992).

5 Conclusions

The classical methodology of characterization of porous solids has been appraised in this paper. Because of inconsistencies in the determination of pore volume, surface area and pore size, we introduce the notion of accessibility into the characterization. As a result, we put forward the definitions of accessible void volume, accessible geometrical surface area and accessible pore size. The new parameters have been demonstrated in a number of model solids whose solid atom configurations are known, and their use is merited through the adsorption properties such as the Henry constant, the isosteric heat at zero loading, the adsorption excess under supercritical conditions. The challenge that now faces us is the experimental determination of these parameters. This will be addressed in our future correspondence.

Acknowledgement Support from the Australian Research Council is gratefully acknowledged.

References

Barker, J., Everett, D.: High temperature adsorption and the determination of the surface area of solids. Trans. Faraday Soc. **58**, 1608–1623 (1962)

Barrett, E., Joyner, L., Halenda, P.: The determination of pore volume and area distributions in porous substances. J. Am. Chem. Soc. **73**, 373–380 (1951)

Birkett, G., Do, D.D.: On the physical adsorption of gases on carbon materials from molecular simulation. Adsorption **13**, 407 (2007)

Broekhoff, J., de Boer, J.: Studies on pore systems in catalysis. J. Catal. **9**, 8–27 (1967)

Broekhoff, J., de Boer, J.: Studies on pore systems in catalysis. J. Catal. **10**, 377–380 (1968a)

Broekhoff, J., de Boer, J.: Studies on pore systems in catalysis. J. Catal. **10**, 391–400 (1968b)

Brunauer, S., Emmett, P.H., Edward, T.: Adsorption of gases in multimolecular layers. J. Am. Chem. Soc. **60**, 309–319 (1938)

Cole, M., Saam, W.: Excitation spectrum and thermodynamics properties of liquid films in cylindrical pores. Phys. Rev. Lett. **32**, 985–988 (1974)

Do, D.D.: Adsorption Analysis: Equilibrium and Kinetics. Imperial College Press, London (1998)

Do, D.D.: Progress in characterization of nanoporous materials: gas phase accessible volume, Henry constant, isosteric heat, solid deformation, accessible pore size and accessible pore volume distribution. In: Invited Lecture at the International Workshop on Frontier Science and Technology of Nanoporous Systems, Chiba, 11–12 July 2008

Do, D.D., Do, H.D.: GCMC surface area of carbonaceous materials with N_2 and Ar adsorption as an alternative to the classical BET method. Carbon **43**, 2112 (2005a)

Do, D.D., Do, H.D.: Adsorption of argon on homogeneous graphitized thermal carbon black and heterogeneous carbon surface. J. Colloid Interface Sci. **287**, 452 (2005b)

Do, D.D., Do, H.D.: Appropriate volumes for adsorption isotherm studies. The absolute void volume, accessible pore volume and enclosing particle volume. J. Colloid Interface Sci. **316**, 317 (2007)

Do, D.D., Birkett, G., Do, H.D.: Adsorption of simple and complex fluids on on-graphitized carbon black and activated carbon—transition from sub-critical to supercritical adsorption and a new method to determine pore size distribution of activated carbon. In: Plenary Lecture at the Carbon Meeting in Seattle (2007)

Do, D.D., Ustinov, E., Do, H.D.: Porous texture characterization from gas-solid adsorption. In: Bottani, E., Tascon, J. (eds.) Adsorption by Carbon, p. 239. Elsevier, Amsterdam (2008a). Chap. 11

Do, D.D., Nicholson, D., Do, H.D.: On the Henry constant and isosteric heat at zero loading in gas phase adsorption. J. Colloid Interface Sci. **324**, 15 (2008b)

Do, D.D., Do, H.D., Wongkoblap, A., Nicholson, D.: Henry constant and isosteric heat at zero-loading for gas adsorption in carbon nanotubes. Phys. Chem. Chem. Phys. **10**, 7293 (2008c)

Do, D.D., Nicholson, D., Do, H.D.: Progress in high pressure methane adsorption in carbonaceous materials. In: Plenary Lecture at the Coal Bed Methane, Brisbane, September 2008d

Do, D.D., Nicholson, D., Do, H.D.: On the anatomy of the adsorption heat versus loading as a function of temperature and adsorbate for a graphitic surface. J. Colloid Interface Sci. **325**, 7 (2008e)

Do, D.D., Herrera, L.F., Do, H.D.: A new method to determine pore size and its volume distribution of porous solids having known atomistic configuration. J. Colloid Interface Sci. **328**, 110 (2008f)

Do, D.D., Wongkoblap, A., Wang, K.: Adsorption of argon, nitrogen and water in carbon nanotube bundles: computer simulation and experimental studies. In: Carbon Conference in Nagano, Japan, July 2008g

Do, D.D., Do, H.D., Nicholson, D.: Molecular simulation of excess isotherm and excess enthalpy change in gas phase adsorption. J. Phys. Chem. B **113**, 1030 (2009)

Duren, T., Millange, F., Ferey, G., Walton, K.S., Snurr, R.Q.: Calculating geometric surface areas as a characterization tool for metal-organic frameworks. J. Phys. Chem. C **111**, 15350 (2007)

Eddaoudi, M., Kim, J., Rosi, N., Vodak, D., Wachter, J., O'Keeffe, M., Yaghi, O.M.: Systematic design of pore size and functionality in

isoreticular MOFs and their application in methane storage. Science **295**, 469 (2002)
Gelb, L.D., Gubbins, K.E.: Langmuir **15**, 305 (1999)
Gregg, S., Sing, K.: Adsorption, Surface Area and Porosity. Academic Press, San Diego (1982)
Herrera, L., Junpirom, S., Do, D.D., Tangsathitkulchai, C.: Computer synthesis of char and its characterization. Carbon **47**, 839 (2009)
Jaroniec, M., Kruk, M., Olivier, J.: Standard nitrogen adsorption data for characterization of nanoporous silicas. Langmuir **15**, 5410–5413 (1999)
Jaroniec, M., Kruk, M., Choma, J.: The 50th anniversary of the BJH method for mesopore analysis: critical appraisal and future perspectives. In: Kaneko, K. (ed.) Fundamentals of Adsorption 7 (2002)
Kanda, H., Myahara, M., Yoshioko, T., Okazaki, M.: Verification of the condensation model for cylindrical nanopores. Langmuir **16**, 6622–6627 (2000)
Kaneko, K.: Determination of pore size and pore size distribution: 1. Adsorbents and catalysts. J. Membr. Sci. **96**, 59–89 (1994)
Kaneko, K., Ishii, C., Kanoh, H., Hanzawa, Y., Setoyama, N., Suzuki, T.: Characterization of porous carbons with high resolution [alpha]s-analysis and low temperature magnetic susceptibility. Adv. Colloid Interface Sci. **76–77**, 295 (1998a)
Kaneko, K., Ishii, U., Kanoh, H., Hanzawa, Y., Setoyama, N., Suzuki, T.: Characterization of porous carbons with high resolution α_s-analysis and low temperature's magnetic susceptibility. Adv. Colloid Interface Sci. **76–77**, 320 (1998b)
Kaneko, K., Ohba, T., Hattori, Y., Sunaga, M., Tanaka, H., Kanoh, H.: Role of gas adsorption in nanopore characterization. Stud. Surf. Sci. Catal. **144**, 11–18 (2002)
Kowalczyk, P., Jaroniec, M., Terzyk, A., Kaneko, K., Do, D.D.: Improvement of the Derjaguin-Broekhoff-de Boer theory for capillary condensation/evaporation of nitrogen in mesoporous systems and its implications for pore size—analysis of MCM-41 silicas and related materials. Langmuir **21**, 1827–1833 (2005)
Kruk, M., Jaroniec, M.: Accurate method for calculating mesopore size distributions from argon adsorption data at 87 K developed using model MCM-41 materials. Chem. Mater. **12**, 222–230 (2000)
Kruk, M., Jaroniec, M.: Argon adsorption at 77 K as a useful tool for the elucidation of pore connectivity in ordered materials with large cagelike mesopores. Chem. Mater. **15**, 2942–2949 (2003)
Neimark, A.V., Ravikovitch, P.: Calibration of pore volume in adsorption experiments and theoretical models. Langmuir **13**, 5148–5160 (1997)
Neimark, A., Ravikovitch, P.: Capillary condensation in MMS and pore structure characterization. Microporus Mesoporus Mater. **44**, 697–707 (2001)
Neimark, A., Ravikovitch, P., Grun, M., Schuth, F., Unger, K.: Pore size analysis of MCM-41 type adsorbents by means of nitrogen andargon adsorption. J. Colloid Interface Sci. **207**, 159–169 (1998)
Neimark, A., Ravikovitch, P., Vishnyakov, A.: Bridging scales from molecular simulations to classical thermodynamics: density functional theory of capillary condensation in nanopores. J. Phys. Chem. Condens. Matter. **15**, 347–365 (2003)
Ravikovitch, P., Neimark, A.: Characterization of nanoporous materials from adsorption, and desorption isotherms. Colloids Surf. A **187**, 11–21 (2001)
Ravikovitch, P., Neimark, A.: Density functional theory of adsorption in spherical cavities and pore size characterization of templated nanoporous silicas with cubic and three dimensional hexogonal structures. Langmuir **18**, 1550–1560 (2002)
Ravikovitch, P., Domhnaill, S., Neimark, A., Schuth, F., Unger, K.: Capillary hysteresis in nanopores: theoretical and experimental studies of nitrogen adsorption on MCM-41. Langmuir **11**, 4765–4772 (1995)
Ravikovitch, P., Haller, G., Neimark, A.: Density functional theory model for calculating pore size distributions. Adv. Colloid Interface Sci. **76**, 203–226 (1998)
Ravikovitch, P., Vishnyakov, A., Russo, R., Neimark, A.: Unified approach to pore size characterization of microporous carbonaceous materials from N2, Ar, and CO2 adsorption isotherms. Langmuir **16**, 2311–2320 (2000)
Reed, T.B., Breck, D.W.: Crystalline zeolites. II. Crystal structures of synthetic zeolite, type A. J. Am. Chem. Soc. **78**, 5972 (1956)
Rouquerol, J., Avnir, D., Fairbridge, C., Everett, D., Haynes, J., Pernicone, N., Ramsay, J., Sing, K.: Recommendations for the characterization of porous solids. Pure Appl. Chem. **66**, 1739–1748 (1994)
Rouquerol, F., Rouquerol, J., Sing, K.: Adsorption by Powder and Porous Solids. Academic Press, San Diego (1999)
Rouquerol, J., et al.: Is the BET equation applicable to microporous adsorbents? In: Studies in Surface Science and Catalysis, pp. 49–56. Elsevier, Amsterdam (2007)
Sing, K., Everett, D., Haul, R., Mouscou, L., Pierotti, R., Rouquerol, J., Siemieniewska, T.: Reporting physisorption data for gas/solid systems with special reference to the determination of surface area and porosity. Pure Appl. Chem. **57**, 603–619 (1985)
Steele, W., Halsey, G.: The interaction of gas molecules with capillary and crystal lattice surfaces. J. Phys. Chem. **59**, 57–65 (1955)
Szostak, R.: Handbook of Molecular Sieves. Van Nostrand Reinhold, New York (1992)
Thommes, M.: Physical adsorption characterization of ordered and amorphous mesoporous materials. In: Lu, G., Zhao, X. (eds.) Nanoporous Materials. Imperial College Press, London (2004)
Thommes, M., Koehn, R., Froeba, M.: Characterization of mesoporous solids. Stud. Surf. Sci. Catal. **142**, 1695–1702 (2000)
Thommes, M., Smarsly, B., Groenewolt, M., Ravikovitch, P., Neimark, A.: Adsorption hysteresis of nitrogen and argon in pore networks and characterization of novel micro- and mesoporous silicas. Langmuir **22**, 756–764 (2006)
Tikhonov, A., Arsenin, V.: Solutions of Ill-Posed Problems. Wiley, New York (1977)
Ustinov, E., Do, D.D., Jaroniec, M.: Equilibrium adsorption in cylindrical mesopores: a modified Broekhoff and de Boer theory versus density functional theory. J. Phys. Chem. B **109**, 1947–1958 (2005)
Ustinov, E., Do, D.D., Jaroniec, M.: Features of nitrogen adsorption on nonporous carbon and silica surfaces in the framework of classical density functional theory. Langmuir **22**, 6238–6244 (2006)
Visnyakov, A., Neimark, A.: Monte Carlo simulation test of pore blocking effects. Langmuir **19**, 3240–3247 (2003)
Walton, K., Snurr, R.: Applicability of the BET method for determining surface areas of microporous metal-organic frameworks. J. Am. Chem. Soc. **126**, 8553 (2007)